Active Sonar Detection in Shallow Water Using the Page Test

Douglas A. Abraham and Peter K. Willett

***Abstract*—The use of active sonar in shallow water results in received echoes that may be considerably spread in time compared to the resolution of the transmitted waveform. The duration and structure of the spreading and the time of occurrence of the received echo are unknown without accurate knowledge of the environment and *a priori* information on the location and reflection properties of the target. A sequential detector based on the Page test is proposed for the detection of time-spread active sonar echoes. The detector also provides estimates of the starting and stopping times of the received echo. This signal segmentation is crucial to allow further processing such as more accurate range and bearing localization, depth localization, or classification. The detector is designed to exploit the time spreading of the received echo and is tuned as a function of range to the expected signal-to-noise ratio (SNR) as determined by the transmitted signal power, transmission loss, approximate target strength, and the estimated noise background level. The theoretical false alarm and detection performance of the proposed detector, the standard Page test, and the conventional thresholded matched filter detector are compared as a function of range, echo duration, SNR, and the mismatch between the actual and assumed SNR. The proposed detector and the standard Page test are seen to perform better than the conventional thresholded matched filter detector as soon as the received echo is minimally spread in time. The use of the proposed detector and the standard Page test in active sonar is illustrated with reverberation data containing target-like echoes from geological features, where it was seen that the proposed detector was able to suppress reverberation generated false alarms that were detected by the standard Page test.**

***Index Terms*—Detection, false alarm performance, Page test, shallow water.**

I. Introduction

N SHALLOW-WATER environments, propagation to the target, reflection off the target, and propagation to the receiver spread an active sonar transmit signal in time and frequency [1]. Traditionally, detection and subsequent range estimation has been performed by thresholding a normalized matched filter output for each of several beams pointing in directions of interest. This is only justifiable as a generalized likelihood ratio test when the received echo is simply a time-shifted scaled version of the transmitted waveform plus white noise, obviously not a realistic scenario in the shallow-water active problem.

Manuscript received June 12, 2000; revised August 2, 2001.

D. A. Abraham was with the NATO SACLANT Undersea Research Centre, La Spezia, Italy. D. Abraham is currently with the Applied Research Laboratory, Pennsylvania State University, State College, PA 16804 USA (e-mail: d.a.Abraham@ieee.org).

P. K. Willett is with the Electrical and Computer Engineering Department, University of Connecticut, Storrs, CT 06269 USA.

Publisher Item Identifier S 0364-9059(02)01616-3.

The primary objective of the detector is to determine if there is a target echo present in the received time series. Subsidiary to detection is the estimation of the starting and stopping times of the echo to be used for subsequent signal processing such as more accurate range and bearing estimation, depth estimation, or classification. Traditionally, signal segmentation is performed by clustering matched filter threshold crossings.

Without exact knowledge of the environment and *a priori* information on the target location and reflection properties, the starting time, duration, and shape of the received echo are unknown, thus hindering design of an optimal receiver. It is, however, desirable to exploit available environmental information to the extent that it can feasibly improve detection performance. Were the optimal detector implementable, it would coherently combine the standard matched filter output according to the multipath structure and the target reflection properties. Baggenstoss [2] has shown that integrating the magnitude-squared matched filter output (i.e., incoherent combination) can improve detection performance in time-spread channels. This paper proposes the use of a sequential detector based on the Page test [3] for active sonar signal detection and segmentation in shallow-water environments. Applied to active sonar detection, the Page test essentially integrates the normalized magnitude-squared matched filter output until it determines that no signal is present, whereupon the process is repeated. A signal-present declaration is made if the integrated sequence exceeds a threshold.

The Page test was originally designed for the detection of a change; for instance, the change from a signal-absent state (hypothesis H_0) to a signal-present state (hypothesis H_1). It may be modified to first look for a change from signal-absence to signal-presence and then to look for a change from signal-presence to signal-absence. This natural extension of the Page test to the detection of multiple finite-duration signals has been described as having alternating hypotheses by Streit [4] and is appropriate for use in the active sonar application. Such a detector will be called an AH-Page test.

Ideally, the log-likelihood ratio (LLR) would be used as the optimal[1] detector nonlinearity in the Page test; that is, the LLR is the optimal transformation of the received data. However, implementation of the LLR requires exact knowledge of the probability density function (PDF) of the normalized matched filter output under H_0 and H_1. A simpler structure is often found in the locally optimal detector nonlinearity, though when using this nonlinearity the Page tests require a false alarm inhibiting bias that is chosen as a function of a design signal-to-noise ratio

[1]Optimal in this case implies minimizing the worst-case average delay before detection when the average time between false alarms is bounded below by some specified value [5], [6].

(SNR). In these situations, the performance of the Page test is often insensitive to mismatch between the actual and assumed SNR, particularly if the actual level exceeds the assumed level. Thus, the SNR may be approximated as a function of range from the transmitter source level, estimates of the transmission loss from acoustic propagation models, estimates of the target strength, and estimates of the reverberation and background noise power level. This *tunes* the detector to look for high SNR signals initially (i.e., short ranges) and low SNR signals later on in the time series (i.e., long ranges). The tuning is accomplished by varying the bias used to hinder false alarms in the Page test. This detector will be called a Page test with signal-strength tuning (SST) to distinguish it from the standard and AH-Page tests where the detector nonlinearity and bias are held constant.

The performance of a detector is usually quantified by the probability of detection and probability of false alarm. These measures are adequate when the detector operates on a fixed amount of data as opposed to sequentially processing an infinite amount of data where, for most detectors, both decisions will occur with probability one. In processing a single ping in an active sonar detection scenario, the fixed amount of data should be chosen to include signal echoes from the maximum range of interest. These data, called a full ping of data, are at most the data between consecutive nonorthogonal waveform transmissions. Additionally, there are opportunities for multiple signal-present declarations (false or otherwise) to be made while processing a full ping of data. Thus, it is proposed that the false alarm performance measure for active sonar signal detectors be the probability of one or more false alarms occurring while processing a full ping of data. This false alarm performance measure provides a measure of how often further action will be required on a per-ping/per-beam basis when no target is present. Though the actual number of false alarms that occur (more specifically, the probability of observing one false alarm, two false alarms, etc.) while processing a full ping of data is also a relevant false alarm performance measure, the above measure is equally meaningful and more tractable analytically.

The Page test has traditionally been analyzed in terms of the average time (or, equivalently, the average number of samples) required before a correct signal-present declaration and between consecutive false signal-present declarations [7]. However, methods exist for determining the probability mass function (PMF)[2] of the stopping time of the Page test [8]–[11]. It will be shown that the probability of one or more false alarms occurring in a full ping of data may be determined from the PMF of the stopping time. The method involving quantization of the Page test statistic update [8], [11] is applied here for determining the PMF of the stopping time and also the probability of detecting a finite duration signal for the proposed SST-Page test. The false alarm performance of the thresholded matched filter, the standard Page test, and the SST-Page test is then compared as a function of range. The detection performance is compared as a function of the signal duration, range, SNR, and the mismatch between the actual SNR and the assumed SNR.

This paper is organized as follows. In Section II, the post-beamformer signal processing, including the normalization scheme, is discussed and the statistical assumptions for the data are described. In Section III. the Page test is introduced and illustrated with a simple example and the SST-Page test is described in detail. In Section IV, the theoretical false alarm and detection performance are evaluated for the proposed detector using the method described in [11]. Finally, as found in Section V, the AH-Page and SST-Page tests are applied to real reverberation data.

[2]The PMF is the equivalent of a probability distribution function for discrete random variables.

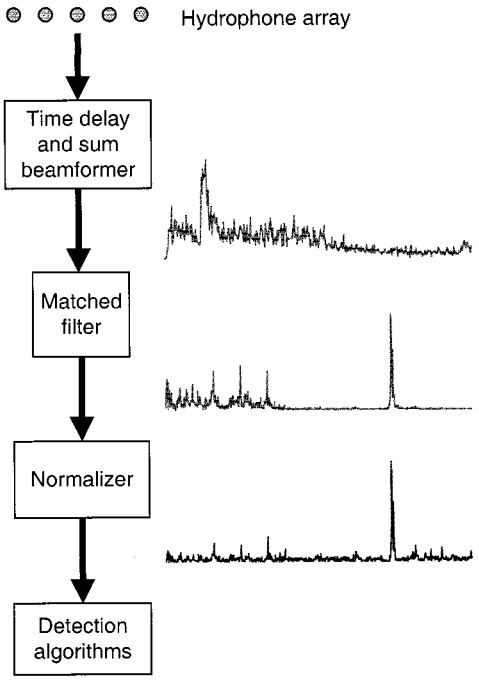

Fig. 1. Flow diagram of processing of array data prior to automatic detection algorithm.

II. Preliminaries

A. Data Preprocessing

Array sensor data are beamformed to a particular direction to increase SNR and attenuate the effects of directional interferences. Active sonar data are typically then matched filtered using the transmitted waveform as a replica. As depicted in Fig. 1, automatic detectors are implemented after the matched filter output has been normalized by estimates of the time-varying reverberation and background noise power.

Let the shape of the transmitted signal be $s[m]$ where m is a time index and $s[m]$ has been scaled to have unit energy

$$\sum_{m=-\infty}^{\infty} |s[m]|^2 = 1. \tag{1}$$

When an echo is present in the received signal, the beamformer output time series may be modeled by

$$x[m] = a[m_t] \sum_{i=1}^{N_p} \gamma_i s[m - m_i] + \sigma_I[m] v[m] \tag{2}$$

where $a[m_t]$ is the echo amplitude assuming the bulk time delay before the echo arrives in m_t samples, $\sigma_I^2[m]$ is the time-varying reverberation and noise power level, and $v[m]$ is a unit-power

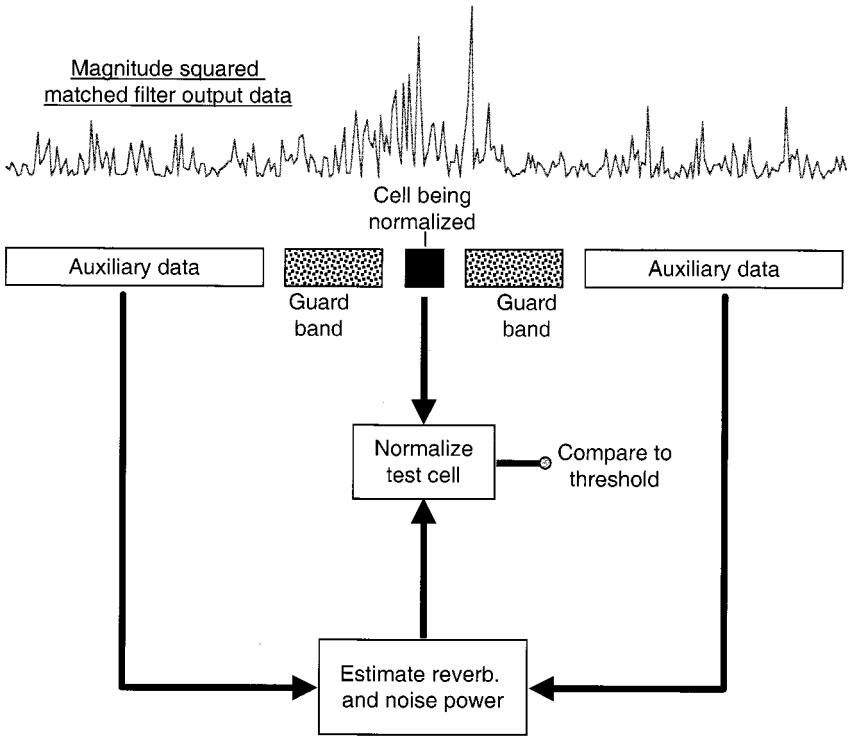

Fig. 2. Flow diagram of the normalization scheme depicting how the reverberation and background noise power is estimated from leading and lagging windows of auxiliary data. A conventional matched filter detector would compare the normalized data to a threshold to declare detection.

Gaussian discrete-time stochastic process. The Gaussianity of $v[m]$ comes from assuming that the reverberation is the result of multiple point scatterers. It is also assumed that the spreading effects of reflection off the target and propagation through shallow water are adequately modeled by a sum over N_p discrete paths with delays m_i and amplitudes γ_i where

$$\sum_{i=1}^{N_p} \gamma_i^2 = 1. \tag{3}$$

The echo parameters ($a[m_t], m_t, m_i, \gamma_i$, and N_p) are dependent on the target position and reflection properties, the receiving array position, and the ocean environment.

Prior to or in conjunction with matched filtering, the beamformer output time series is basebanded by the center frequency of the transmit signal, low-pass filtered, and decimated to a sampling frequency equal to the bandwidth of the transmitted signal. The matched filter output may then be described by

$$\begin{aligned} y[n] &= a[n_t] \sum_{i=1}^{N_p} \gamma_i r_{ss}[n - n_i] + \sigma_I[n] w[n] \\ &= \tilde{a}[n, n_t] + \sigma_I[n] w[n] \end{aligned} \tag{4}$$

where $r_{ss}[n]$ is the autocorrelation sequence of the basebanded, filtered, and decimated transmit signal, n_t is the decimated bulk delay of the echo, n_i are the decimated path delays, and $w[n]$ is now assumed to be a unit-power, white, complex Gaussian discrete-time stochastic processes. Under reverberation limited conditions, the whiteness of the noise may not be a reasonable assumption. The optimal filter, as described by Van Trees [12], involves deconvolving the transmitted signal and requires knowledge of the scattering function. These assumptions should not be too detrimental except perhaps when the reverberation spectrum is distinctly nonwhite or if the reverberation is not substantially due to multiple point scatterers. In the latter situation, if the statistical distribution of the reverberation is known or can be estimated, transformation of the data by an LLR or locally optimal nonlinearity may improve performance.

B. Normalization

Automatic detection algorithms require normalization to produce test statistics that follow a known probability distribution when no echo is present, allowing the detector thresholds to be chosen according to a desired false alarm performance specification. As shown in Fig. 2, normalization is accomplished by estimating the reverberation and background noise power from auxiliary data adjacent in time to the cell being normalized. The conventional thresholded matched filter detector declares that a target is present when the normalized data exceeds a threshold.

As the normalizer slides through the matched filter output in time, the auxiliary data will be corrupted by data containing signal. Guardbands are used to help isolate the auxiliary data from contamination by the signal when spreading in time is expected. There exist several methods for forming robust estimates of the reverberation and background noise power from contaminated auxiliary data [13], [14]. The trimmed-mean (TM) normalizer described by Gandhi and Kassam [13] is used in processing the data presented in this paper.

The TM-normalizer estimates the reverberation and background noise power by forming the mean after discarding some of the largest and some of the smallest samples of the magnitude squared auxiliary data. Suppose the leading and

lagging windows of auxiliary data are each M samples long and together provide the magnitude squared data $V_1, \ldots, V_{2M}$. These samples are then ordered by their magnitude to produce the data $V_{(1)} < V_{(2)} < \cdots < V_{(2M)}$. The estimate of the reverberation and background noise power using the TM-normalizer has the form

$$\hat{\sigma}^2 = \frac{1}{c(i_0, i_1, 2M)} \sum_{i=i_0}^{i_1} V_{(i)}. \tag{5}$$

The indices i_0 and i_1 $(1 \leq i_0 \leq i_1 \leq 2M)$ describe the TM-normalizer. The scale factor is chosen so that the estimator is unbiased. If the magnitude squared auxiliary data are exponentially distributed with mean σ^2, as will be the case under the Rayleigh reverberation assumption, this results in

$$c(i_0, i_1, 2M) = \frac{1}{\sigma^2} E\left[\sum_{i=i_0}^{i_1} V_{(i)}\right] = \sum_{i=1}^{i_1} \frac{i_1 - \max(i, i_0) + 1}{2M - i + 1}. \tag{6}$$

The matched filter output for the test cell is then normalized according to

$$z[n] = 2\frac{|y[n]|^2}{\hat{\sigma}^2[n]}. \tag{7}$$

The normalization process alters the statistical distribution of the data by introducing correlation in time and increasing the tail of the distribution. The theoretical analyses in this paper assume ideal normalization, which results in a noncentrally chi-squared distribution

$$z[n] \sim \mathcal{X}_2^2(\delta_z[n]) \tag{8}$$

with two degrees of freedom and noncentrality parameter

$$\delta_z[n] = 2\frac{|\tilde{a}[n, n_t]|^2}{\sigma_I^2[n]}. \tag{9}$$

III. The Page Test Applied to Active Sonar Detection

The basic Page test [3] was designed to detect a change in the distribution of a sequence of data. The Page test declares signal presence when the statistic

$$W_n = \max\{0,\, W_{n-1} + g(z[n])\} \tag{10}$$

crosses a threshold where $W_0 = 0$ and the detector nonlinearity $g(z)$ is ideally the LLR of the observed data $z[n]$.

In active sonar, the detector must search for multiple limited-duration changes in the distribution of the normalized matched filter output. This may be accomplished with the Page test by consecutively searching for the onset of a signal and then searching for its termination. Streit [4] has termed such an implementation of the Page test as having alternating hypotheses, that is, the AH-Page test.

An example of the test statistic (i.e., W_n) for an AH-Page test is found in Fig. 3. For this example, constant level signals were added to zero-mean, unit-variance, Gaussian noise at time samples 100 and 200, respectively, with durations of 10 and 50 samples and levels of 2 and 1. The detection of the onset and termination of the first signal is indicated on the figure at the appropriate threshold crossing. The second signal is detected, but suffers a long delay prior to detection owing to its weaker level. This is typical of the Page test in that, on average, it takes more samples to detect weaker signals than it does stronger ones. As described in [15] and noted on the figure, the starting and stopping time of the signal may be estimated from the test statistic. As one would expect, the quality of the estimates improves with SNR. The example seen in Fig. 3 illustrates this point in that the starting and stopping time estimates for the stronger signal are accurate and the starting time estimate of the weaker signal has significant error.

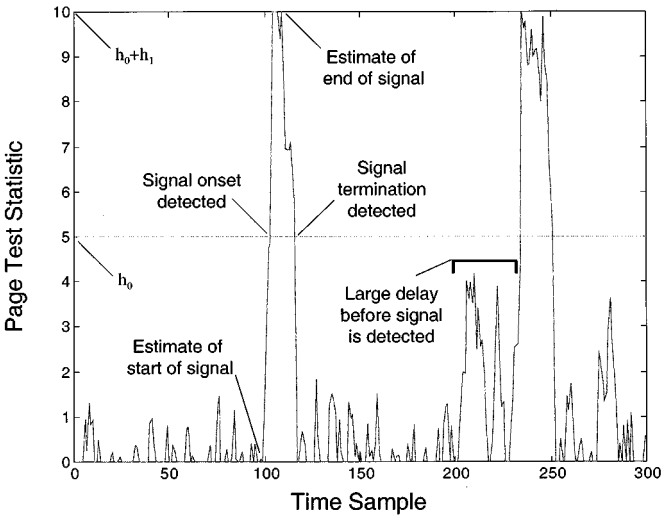

Fig. 3. Example of the operation of the AH-Page test in detecting signals of varying duration in noise: the test statistic is shown as a function of time sample.

A. Detector Nonlinearity

In the Page test, the LLR is the optimal detector nonlinearity in the sense of minimizing the worst-case average delay before detection while constraining the average time between false alarms. However, it does not necessarily maximize the probability of detecting a finite duration signal.

Implementation of the LLR requires knowledge of the PDF of the data under both the signal-present and signal-absent hypotheses. To avoid requiring explicit knowledge about the signal, the locally optimal detector nonlinearity is often used, providing near optimality for weak signals and usually a simpler structure. For a noncentral chi-squared distributed signal, the locally optimal nonlinearity is simply the data itself

$$g(z) = z - b \tag{11}$$

where b is a false alarm inhibiting bias required by the Page test. The bias may be chosen to maximize the asymptotic performance [16]

$$b = L\left(1 + \frac{L}{\tilde{\delta}}\right)\log\left(1 + \frac{\tilde{\delta}}{L}\right) \tag{12}$$

or in a simpler fashion using Dyson's method [16]

$$b = L + \frac{\tilde{\delta}}{2} \tag{13}$$

where L is the number of degrees of freedom of the chi-squared distribution and $\tilde{\delta}$ is a design noncentrality parameter.

As seen in (9), the noncentrality parameter of the chi-squared distribution is twice the SNR. The design noncentrality parameter should be chosen using as accurate an estimate of the SNR as possible. The sonar equation [1] provides a method for approximating the SNR of an echo

$$\mathrm{SNR}_{\mathrm{dB}}[n] = \mathrm{SL}_{\mathrm{dB}} - \mathrm{TL1}_{\mathrm{dB}}[n] - \mathrm{TL2}_{\mathrm{dB}}[n] + \mathrm{TS}_{\mathrm{dB}} - \mathrm{RL}_{\mathrm{dB}}[n] \quad (14)$$

where $\mathrm{SL}_{\mathrm{dB}}$ is the source level, $\mathrm{TS}_{\mathrm{dB}}$ is the target strength, $\mathrm{RL}_{\mathrm{dB}}[n]$ is the range-dependent reverberation level at the output of the matched filter, and $\mathrm{TL1}_{\mathrm{dB}}[n]$ and $\mathrm{TL2}_{\mathrm{dB}}[n]$ represent the range-dependent transmission loss from transmitter to target and target to receiver.

The transmission loss may be estimated from empirical models such as Marsh and Schulkin's (described by Urick [1, pp. 177–179]) or by using more complicated models such as the SACLANT Centre normal-mode acoustic propagation model (SNAP) [17]. The target strength should be chosen according to the minimum level expected to be observed. The reverberation power level may be obtained from the estimate used to normalize the data. Thus, the design noncentrality parameter used to tune the Page test to the strength of the target echo has the form

$$\tilde{\delta}[n] = 2 \cdot 10^{(\mathrm{SNR}_{\mathrm{dB}}[n]/10)} \quad (15)$$

with the parameters of the sonar equation estimated as described.

It is prudent to require that $\mathrm{SNR}_{\mathrm{dB}}[n]$ be greater than a minimum level so the detector does not search for vanishingly small signals as range increases, thus producing false alarms.

B. Detection and Segmentation Algorithm

The following describes the SST-Page test, essentially an extension of an AH-Page test. Included in the description are estimators for the starting (n_s) and stopping times (n_e) of the signal as described in [15]. The threshold (h_0) and detector nonlinearity $(g_n^0(z))$ for the Page test searching for the onset of a signal are different from those (h_1 and $g_n^1(z)$) for the Page test searching for the termination of the signal. This allows independent control of the probability of falsely declaring that a signal has started and falsely declaring that a signal has ended. The detector nonlinearities are described as being time-variable. This allows incorporation of the time-varying design noncentrality parameter, resulting in the SST-Page test:

(1) Set $W_0 = 0$, $n = 1$, $n_s = 0$.
(2) If $W_{n-1} < h_0$,
- Set $W_n = \max\{0, W_{n-1} + g_n^0(z[n])\}$.
- If $W_n = 0$, set $n_s = n$.
- If $W_n < h_0$, set $n = n+1$ and goto (2)

Else (i.e., if $W_n \geq h_0$),
- The leading edge of a signal has been detected.
- An estimate of the starting time index is n_s.
- Set $W_n = h_0 + h_1$, $n_e = n$, $n = n+1$, and goto (3)

(3) If $W_{n-1} \geq h_0$,
- Set $W_n = \min\{h_0 + h_1, W_{n-1} + g_n^1(z[n])\}$.
- If $W_n = h_0 + h_1$, set $n_e = n$.
- If $W_n > h_0$, set $n = n+1$ and goto (3)

Else (i.e., if $W_n \leq h_0$),
- The lagging edge of a signal has been detected.
- An estimate of the stopping time index is n_e.
- Set $W_n = 0$, $n_s = n$, $n = n+1$ and goto (2)

IV. Theoretical Performance Analysis

Signal detectors are typically compared by first designing them to have equivalent false alarm performance and subsequently comparing their detection performance. The detection performance is commonly and appropriately defined as the probability of a detection occurring due to the presence of a signal. In processing a full ping of active sonar data where the signal only occupies a portion of the data being processed, this is interpreted to mean the probability of a detection when the test statistic exceeding the threshold is formed from data that includes some part of the signal.

The false alarm performance may be quantified in a variety of ways. As there is opportunity for multiple false alarms within one ping of active sonar data, the probability of one or more false alarms is adopted as the false alarm performance measure. This measure is nearly equivalent to the probability of one false alarm occurring when that probability is very small and more appropriately represents the occurrence of false alarms in active sonar signal processing.

A. False Alarm Performance

Define the integer-valued random variable N as the first stopping time of an active sonar echo detector, that is, the time index of the first signal-present declaration while processing a full ping of data. The PMF of N, $f_N(n)$, provides a complete description of the false alarm performance of a detector given a specific threshold. Most false alarm performance measures attempt to describe a pertinent univariate characteristic of the complete description provided by $f_N(n)$. Unfortunately, it is often difficult to obtain analytical forms for $f_N(n)$ and simulation may be prohibitive for more than a single threshold value [10]. However, analytical or computational solutions do exist for certain detector structures.

The above false alarm performance measure can be described in terms of both the PMF of N and its cumulative distribution function (CDF)

$$F_N(n) = \sum_{i=1}^{n} f_N(i). \quad (16)$$

Let $\alpha(N_{\max})$ be the probability of one or more false alarms occurring while processing a ping of data $N_{\max}$ samples long. Clearly $\alpha(N_{\max})$ is also equal to one minus the probability of no false alarms occurring in $N_{\max}$ samples, which is related to the PMF and CDF of N as follows:

$$\begin{aligned}\alpha(N_{\max}) &= 1 - \Pr\{\text{No false alarms in } N_{\max} \text{ samples}\} \\ &= 1 - \Pr\{N \nleq N_{\max}\} \\ &= \sum_{n=1}^{N_{\max}} f_N(n) \\ &= F_N(N_{\max}). \end{aligned} \tag{17}$$

1) Thresholded Matched Filter: Consider the detector implemented by comparing the matched filter output normalized by the reverberation and background noise power to a threshold. Assume that the normalized matched filter output, $\{z[n]\}_{n=1}^{N_{\max}}$, consists of independent and identically distributed (i.i.d) random variables when no signal is present. This assumption is not realistic when the reverberation and noise background power level is estimated from auxiliary data nearby in the matched filter time series and only approximately true, as previously mentioned, in reverberation limited conditions. However, it provides an approximate analysis.

Let the CDF of $z[n]$ be $F_0(\tau) = \Pr_0\{z[n] < \tau\}$ when no signal is present. The stopping time N is the first time that a sample crosses the threshold h_0

$$N = \min\{n: z[n] > h_0 \text{ and } 0 < n \leq N_{\max}\}. \tag{18}$$

The probability that $N = n$ for $n \geq 1$ is equal to the probability that the first $n-1$ samples are below the threshold and that the nth sample is above the threshold

$$f_N(n) = p^{n-1}(1-p) \tag{19}$$

where $p = \Pr_0\{z[n] < h_0\} = F_0(h_0)$. Equation (19) may be recognized as the PDF of a geometric random variable. The geometric random variable is a special case of the negative binomial distribution [18] which is derived from the number of trials before a specific event occurs.

The CDF of N is, in this case,

$$F_N(n) = \sum_{i=1}^{n} f_N(i) = 1 - p^n \tag{20}$$

and the probability of one or more false alarms while processing a ping of data is

$$\alpha(N_{\max}) = 1 - p^{N_{\max}}. \tag{21}$$

Assuming that the normalized matched filter output is centrally chi-squared distributed with two degrees of freedom (i.e., ideal normalization), the CDF is $F_0(z) = 1 - e^{-(z/2)}$ for $z \geq 0$. Substitution of this assumption into (21) followed by functional inversion results in the following relationship between the detector threshold (h_0) and the false alarm performance:

$$h_0 = -2\log\left\{1 - [1 - \alpha(N_{\max})]^{1/N_{\max}}\right\}. \tag{22}$$

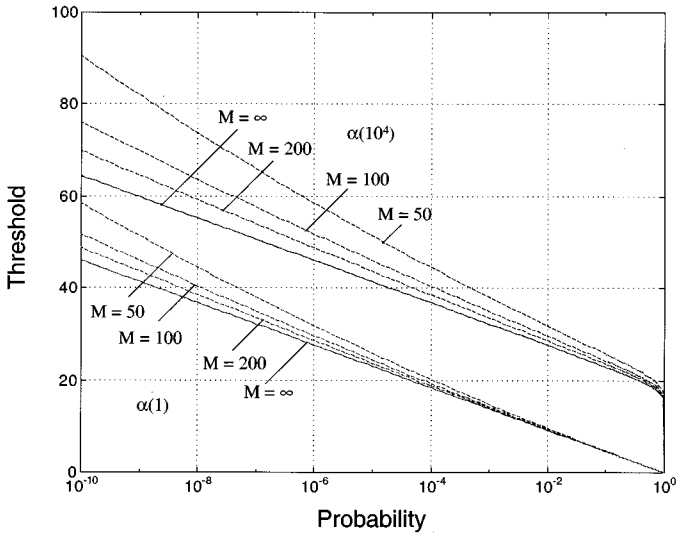

Fig. 4. Matched filter threshold as a function of false alarm performance measures for chi-squared (solid lines) and F (dashed lines) distributions.

Cell averaging constant false alarm rate (CA-CFAR) systems normalize the matched filter output cell being tested by the mean of auxiliary data taken from leading and lagging windows. Under H_0, this results in a central F distribution with 2 and $2M$ degrees of freedom where M is the total number of auxiliary data samples in the leading and lagging windows. Multiplying this statistic by 2 creates one that tends to a chi-squared distribution with two degrees of freedom as the amount of auxiliary data increases to infinity. The CDF of this scaled and normalized matched filter output is $F_0(z) = 1 - (1 + (z/2M))^{-M}$ for $z \geq 0$. The resulting relationship between the false alarm performance and the detector threshold is

$$h_0 = 2M\left\{\left[1 - [1 - \alpha(N_{\max})]^{1/N_{\max}}\right]^{-1/M} - 1\right\}. \tag{23}$$

By letting $M \to \infty$, (23) goes to (22), as seen in Fig. 4 where the detector threshold is shown as a function of the false alarm performance for $N_{\max} = 1$ and $N_{\max} = 10^4$ for various values of M. From this figure, it is also seen that choosing the threshold so that $\alpha(10^4) = 10^{-4}$ is equivalent to choosing $\alpha(1) \approx 10^{-8}$. More complicated normalization algorithms such as those utilizing order statistics can improve the robustness of the normalization to signal presence or outliers at the expense of a more difficult, although not impossible, analysis.

2) Page Tests: Traditionally, the false alarm performance of the Page test has been described by the average time between false alarms. However, methods exist for determining the PMF and CDF of the stopping time [8]–[11]. The method described in [8] and [11] is of particular interest because it may be applied to the Page test with signal-strength-tuning for determining false alarm and detection performance and is accurate to within the error introduced by quantization of the update statistic.

The SST-Page test differs from the standard Page test in two respects: a time-varying detector nonlinearity and an alternating-hypothesis implementation. The false alarm performance of the AH-Page test, as quantified by the probability of one or more false alarms in $N_{\max}$ samples, is equivalent to

that of the standard Page test. This results from the dependence of the false alarm performance solely on the PMF of the *first* stopping time of the AH-Page test,

$$N = \min\{n: W_n > h_0 \text{ and } 0 < n \leq N_{\max}\}. \quad (24)$$

This statement holds with or without the time-varying detector nonlinearity.

As described in [11], calculation of the CDF of the stopping time requires quantization of the update $g_n^0(z)$ to the Page test and formation of a probability transition matrix. The derivation, which is a straightforward extension of [11] simply accounting for the time-varying nature of the detector nonlinearity, is found in Appendix I and results in

$$F_N(n) = 1 - \mathbf{1}^T \mathbf{C}_n \mathbf{C}_{n-1} \mathbf{C}_{n-2} \cdots \mathbf{C}_1 \mathbf{u}_0 \quad (25)$$

where $\mathbf{C}_n$ is the probability transition matrix, $\mathbf{1}$ is a vector of ones, $\mathbf{u}_0$ is a vector composed of the initial probabilities of observing the continuing states, and the superscript T represents the transpose operation. In the active sonar problem, the detector will start from the zero state so $\mathbf{u}_0$ is a vector with a one in the first position and zeros elsewhere (say $\mathbf{e}_0$).

When the detector nonlinearity does not change with time, (25) may be simplified [11] to a function involving the eigenvalues and eigenvectors of the now constant probability transition matrix, say $\mathbf{C}_0$. Let $\mathbf{C}_0$ have eigendecomposition $\mathbf{C}_0 = \mathbf{Q}\Lambda\mathbf{Q}^{-1}$ where Λ is a diagonal matrix of the eigenvalues λ_1, $\lambda_2, \ldots, \lambda_\gamma$. Let the vector $\mathbf{r}$ be the Schur product (i.e., element by element multiplication) of the vectors $\mathbf{Q}^T\mathbf{1}$ and $\mathbf{Q}^{-1}\mathbf{u}_0$. Then, as shown in [11], the CDF of the stopping time N is

$$F_N(n) = 1 - [\lambda_1^n \quad \lambda_2^n \quad \ldots \quad \lambda_\gamma^n]\mathbf{r} \quad (26)$$

and the false alarm performance is

$$\begin{aligned}\alpha(N_{\max}) &= 1 - \mathbf{1}^T \mathbf{C}_0^{N_{\max}} \mathbf{u}_0 \\ &= 1 - [\lambda_1^{N_{\max}} \quad \lambda_2^{N_{\max}} \quad \ldots \quad \lambda_\gamma^{N_{\max}}]\mathbf{r}. \quad (27)\end{aligned}$$

Equations (26) and (27) describe the false alarm performance of the standard Page test and the AH-Page test. They may be used as an upper bound on the performance of the SST-Page test if the matrix $\mathbf{C}_0$ is chosen when the detector nonlinearity assumes the weakest signal, that is, when it is easiest for the detector to produce a false alarm. It is recommended that the thresholds required for implementation of the detector (h_0 and h_1) be chosen using this bound—to do otherwise requires exorbitant computation.

The threshold required to implement the Page test is shown in Fig. 5 as a function of $\alpha(n)$ for $n = 1, 10, 10^2, \ldots, 10^6$ when the bias is chosen according to a design SNR of 10 dB and ideal normalization is assumed. Here it is observed that choosing $\alpha(10^4) = 10^{-4}$ is approximately equivalent to choosing $\alpha(1) = 10^{-9}$.

3) Comparison: Suppose that a full ping of data consists of 10^4 time samples. If the sampling rate were 500 Hz, this would include targets out to approximately 15 km in range assuming a 750-m/s two-way propagation speed. The thresholds required to implement the thresholded matched filter and the Page tests are set so the probability of at least one false alarm in 10^4 samples is $\alpha(10^4) = 10^{-4}$. The threshold obtained for the standard Page test with a detector nonlinearity assuming the weakest signal is used for the Page test with signal-strength tuning. The PMF and CDF of the stopping time as a function of time sample are found in Fig. 6.

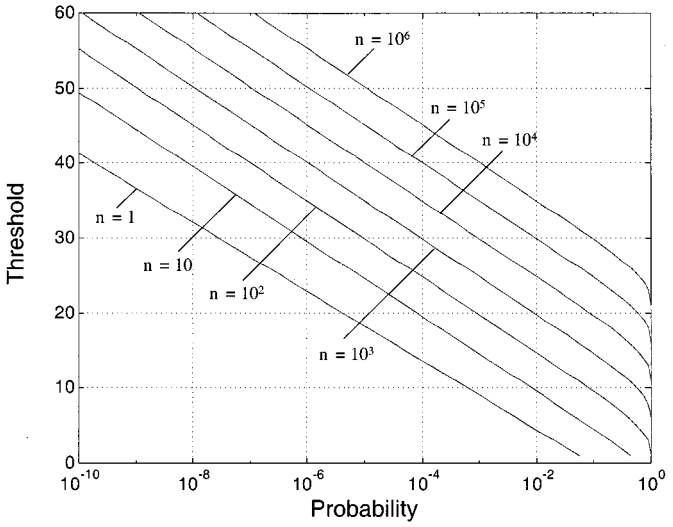

Fig. 5. Page test threshold as a function of $\alpha(n)$ for various values of n.

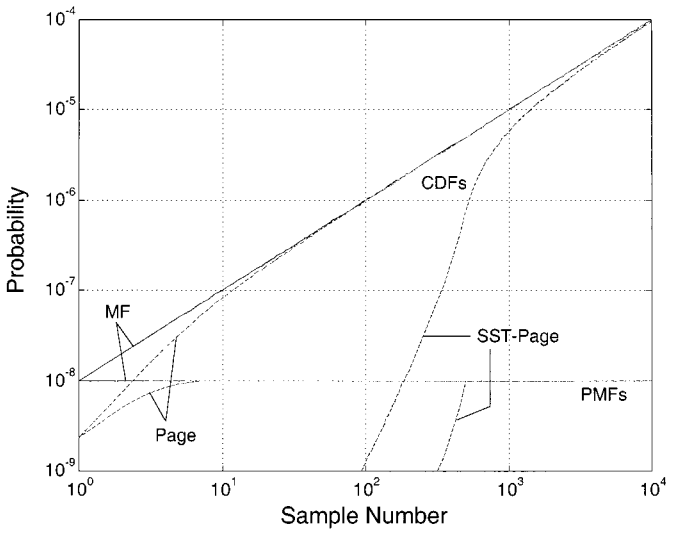

Fig. 6. PMF and CDF of stopping time as a function of sample number for thresholded matched filter, standard Page test, and SST-Page test.

The semi-empirical transmission loss approximation of Marsh and Schulkin, as described by Urick [1], was used to tune the SST-Page test with the asymptotically optimal bias and $\mathrm{SL}_{\mathrm{dB}}$ and $\mathrm{TS}_{\mathrm{dB}}$ chosen so $\mathrm{SNR}_{\mathrm{dB}}[n = 500] = 10$ dB. Beyond 500 samples, the bias for the SST-Page test was chosen according to an SNR of 10 dB. The improved false alarm suppression capability (i.e., lower PMF and CDF) of the SST-Page test over the standard Page test and thresholded matched filter is evident at short ranges.

B. Detection Performance

As previously mentioned, the detection performance is quantified by the probability of detecting a signal when the decision occurs due to signal presence. Ideally, detailed acoustic and

target models would be used to determine the time spreading and shape of a received target signal in specific shallow-water environments (i.e., the function $\tilde{a}[n, n_t]$) from which the detection performance of the thresholded matched filter and Page tests may be determined. However, to provide an idea of how the detectors perform in a less specific scenario, a simple model is considered where a signal with constant SNR starts at time sample n_s and ends after time sample n_e. The detection performance of the aforementioned more realistic target echoes would be similar, though not identical, to that observed in Sections IV-B1–IV-B3 were they quantified by their duration and average SNR.

1) Thresholded Matched Filter: An echo is considered detected by the thresholded matched filter if at least one threshold crossing occurs throughout the extent of the signal. This is equivalent to one minus the probability that no threshold crossings occur. Suppose that the CDF of the normalized matched filter output is $F_1(z|\delta_z[n])$ where $\delta_z[n]$ is the noncentrality parameter of (9). The detection probability is then

$$P_d(L) = 1 - \prod_{n=n_s}^{n_e} F_1(h_0|\delta_z[n]) \tag{28}$$

where $L = n_e - n_s + 1$ is the duration of the signal. When the noncentrality parameter is constant (δ_z) throughout the duration of the signal, the probability of detection simplifies to

$$P_d(L) = 1 - [F_1(h_0|\delta_z)]^L. \tag{29}$$

As previously mentioned, the normalized matched filter output is noncentrally chi-squared distributed under the perfect normalization assumption. CA-CFAR processing results in a noncentral F distribution with noncentrality parameter $\delta_z[n]$ and, as before, 2 and $2M$ degrees of freedom. The CDFs for these distributions are most easily determined by approximation; of note are the two- and three-moment approximations described by Johnson and Kotz [19], [20] which are easily implemented and perform well.

2) Page Tests: If the detector nonlinearity and false alarm inhibiting bias remain approximately constant throughout the duration of the signal, the probability of detecting a finite duration signal using the SST-Page test will be very close to the probability of detection using the standard Page test. As described in [11], the probability of detecting a finite duration signal using the Page test is bounded below by the CDF of the stopping time evaluated at the duration of the signal. The CDF of the stopping time is a bound because it does not account for latent detections, which are detections that occur after the signal has ended but prior to a reset of the Page test statistic to zero. As mentioned in [11], the probability of a latent detection may be determined using the quantization-based solution to the CDF of the stopping time. The reader is referred to Appendix II for the derivation and presentation of the probability of detection using the Page test including latent detections.

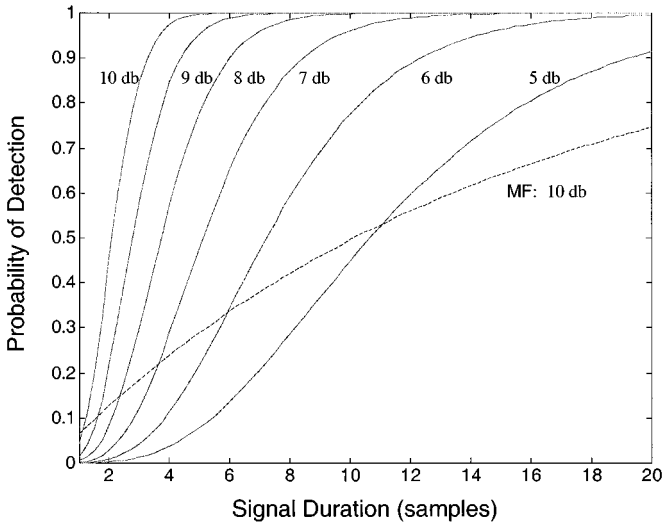

Fig. 7. P_d versus signal duration for various SNRs and a 10-dB design SNR.

3) Comparison: In the following P_d analyses, the thresholds were chosen so that $\alpha(10^4) = 10^{-4}$ assuming perfect normalization. The performance of the detectors is described as a function of the SNR at the matched filter output which is half of the noncentrality parameter of the noncentral chi-squared or F distributions.

The expected increase in P_d as the signal duration increases is observed for the Page test in Fig. 7 for several SNRs when the asymptotically optimal bias is chosen according to a design SNR of 10 dB. When the actual SNR is less than the assumed SNR (all the solid curves with $\mathrm{SNR} < 10$ dB), detection performance is reduced, particularly for short duration signals. The P_d for the thresholded matched filter is shown in Fig. 7 only for the 10-dB SNR case (dashed line). Comparing this curve with the 10-dB SNR case of the Page test, it is seen that the Page test has better performance except for extremely short duration signals. This highlights the fact that, when the signal only exists for a very short time (e.g., one or two samples), there is not much gained by the integration inherent in the Page test and thus the thresholded matched filter performs better. However, in most shallow-water environments, the acoustic propagation will induce enough spreading of the target echo to be in the region where the Page test outperforms the thresholded matched filter.

The increase in P_d as a function of SNR for the Page test with various design SNRs is shown in Fig. 8 for a signal five samples long. Here it is seen that when the design SNR is large, detection is hindered for weaker signals. This implies that early on in the matched filter time series (i.e., short ranges), where the design SNR is large, the SST-Page test may not produce false alarms due to signal-like reverberation where the thresholded matched filter would.

Fig. 9 illustrates how P_d changes with range for various SNRs when the signal duration is five samples and the bias is chosen according to the estimated noncentrality parameter as described in Section IV-A3 for the false alarm performance comparison. The P_d for the thresholded matched filter, which is constant with range, is shown on each curve where it is seen that the SST-Page test automatically inhibits detection for short ranges, except for strong signals, and encourages detection for longer ranges.

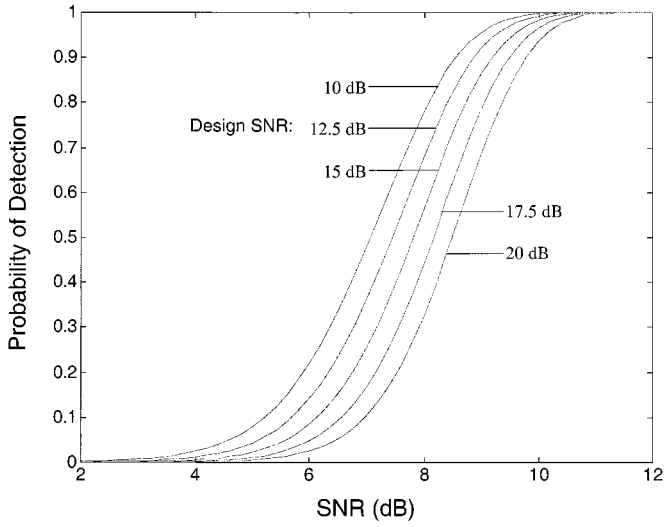

Fig. 8. P_d of a signal five samples long versus SNR for various design SNRs.

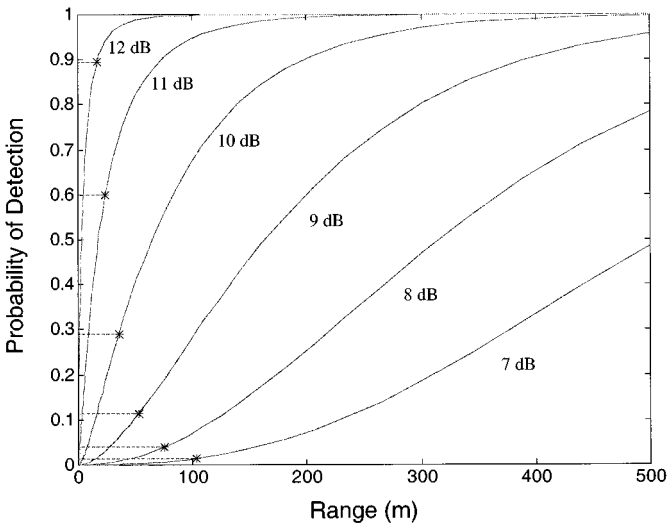

Fig. 9. P_d of a signal five samples long versus range for various SNRs. Conventional matched filter P_d, which is constant with range, is shown on each curve for the same SNRs.

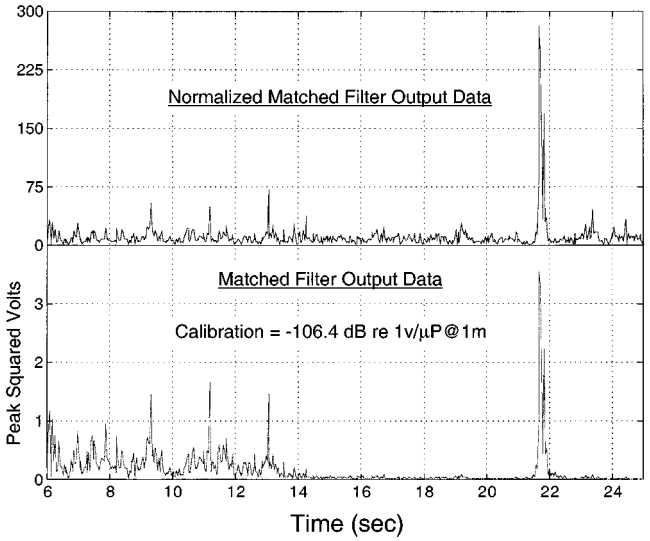

Fig. 10. Matched filter output before and after normalization.

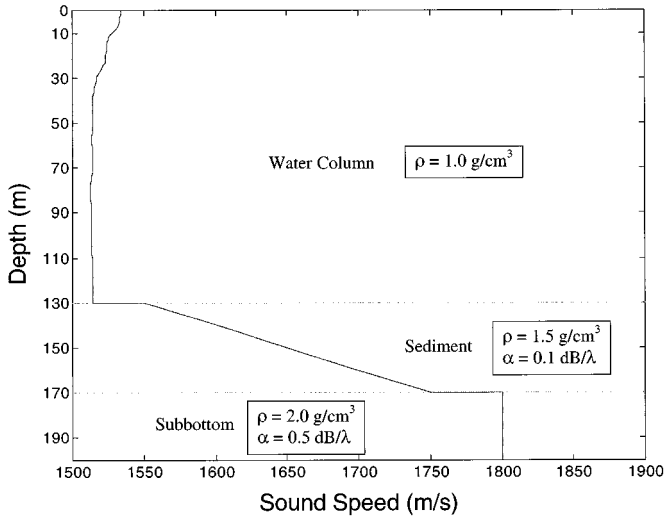

Fig. 11. Description of environment.

V. Real Data Example

To demonstrate the effectiveness of the SST-Page test, a sample of reverberation data has been processed. The data are known to contain reflections from a subseafloor geological feature [21]. The matched filter output before and after normalization is shown in Fig. 10 where the subseafloor reflector is seen to provide a very strong return just prior to 22 s. Additionally, there are several peaks earlier in the time series that do not have any known geological features associated with them and are considered to be clutter-generated false alarms.

For the purpose of estimating the transmission loss, the environment was assumed to be a range-independent acoustic waveguide with a uniform depth of 130 m, a 40-m sediment layer, and a semi-infinite subbottom. The water column, sediment, and subbottom layer sound-speed profiles, densities, and attenuations are found in Fig. 11. The subbottom shear attenuation was assumed to be 1.5 decibels per wavelength (dB/λ) and the subbottom shear speed was assumed to be 450 m/s. SACLANT Centre's normal mode acoustic propagation model (SNAP) [17] was used to determine the transmission loss. As the depth of the target is unknown, the transmission loss is approximated by averaging over depth with equal weighting for each depth point. It may be more appropriate to apply a higher weighting to depths the target is expected to frequent. The depth averaged transmission loss curves from SNAP for the source to target and target to receiver legs are shown in Fig. 12. The difference between the curves is due to the differing depths of the transmitter (78 m) and the receiver (65 m).

Utilizing a source level of 230 dB//1 μP@1 m, a target strength of 10 dB, the depth averaged transmission loss estimates from SNAP, and the reverberation power level as estimated by the normalizer, (14) is used to form the design SNR for the SST-Page test. The result is displayed in Fig. 13 and seen to vary from almost 22 dB down to the minimum allowable value of 10 dB.

An AH-Page test with a design SNR of 10 dB, Dyson's bias, and thresholds $h_0 = h_1 = 45$ was applied to the data. This combination results in a false alarm performance of $\alpha\left(10^4\right) < 10^{-6}$

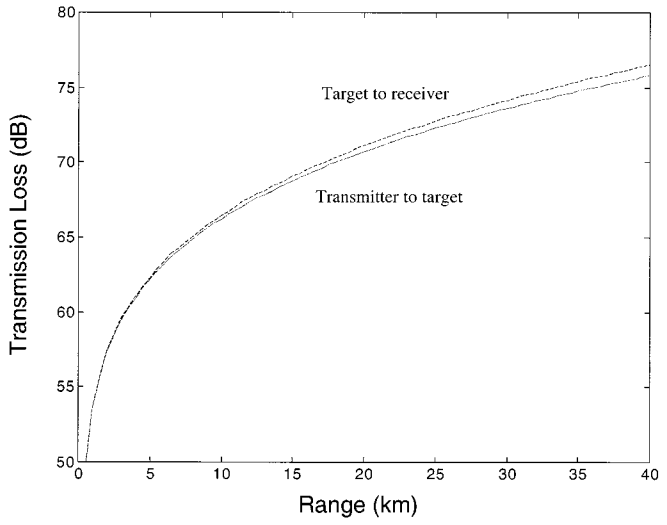

Fig. 12. Depth averaged transmission loss from SNAP at 650 Hz.

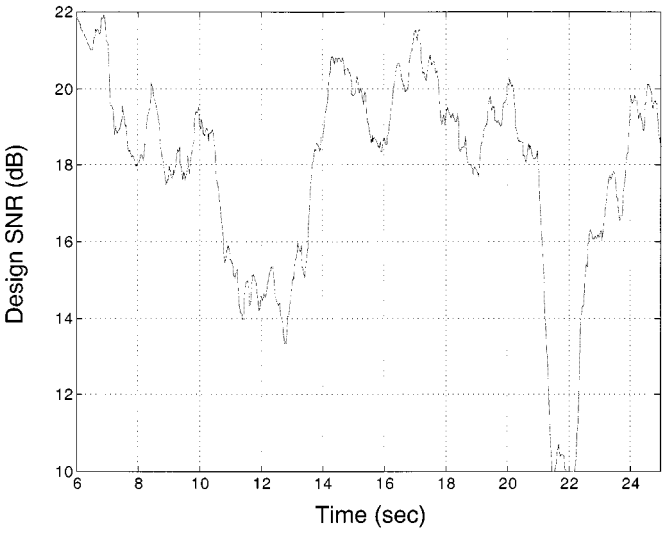

Fig. 13. Design SNR as estimated from source level, assumed target strength of 10 dB, depth averaged transmission loss estimates, and estimates of reverberation power from normalizer. A minimum value of 10 dB was enforced on the design SNR.

when the reverberation is Rayleigh and the normalization is perfect. The resulting Page test statistic and detector state are displayed in Fig. 14. The detector state displays the results of estimating the starting and stopping times of the signals detected by the Page test. As seen on the figure, two of the spikes observed in the normalized matched filter data have been detected along with the subseafloor reflector just before 22 s.

The SST-Page test with the design SNR shown in Fig. 13 is applied to the same data. The results displayed in Fig. 15 show that the spikes early on in the time series are suppressed while the subseafloor reflector just before 22 s is still detected. Figs. 16 and 17 contain an enlargement of the region around the subseafloor reflector—illustrating the performance of the SST-Page test in detecting and segmenting the echoes.

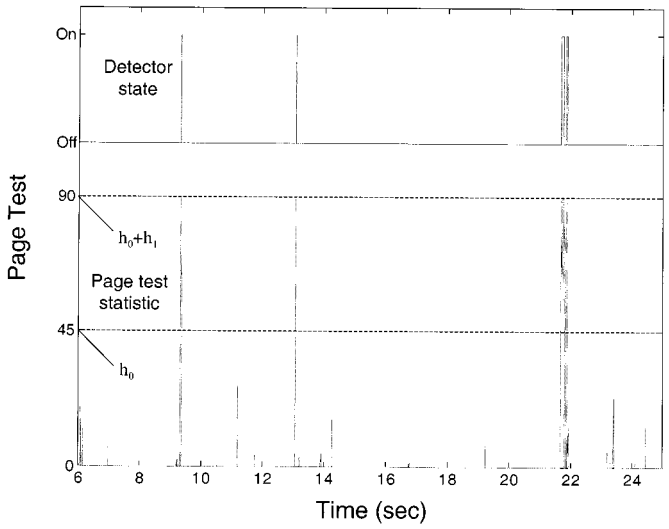

Fig. 14. Results of AH-Page test with a 10-dB design SNR.

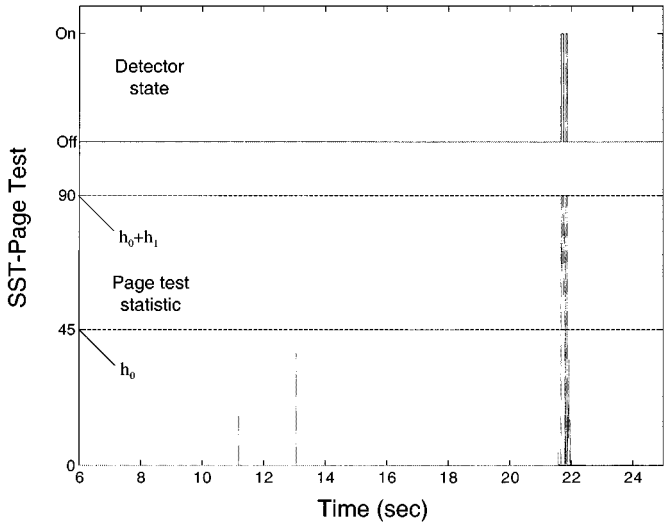

Fig. 15. Results of SST-Page test with design SNR estimated from sonar equation.

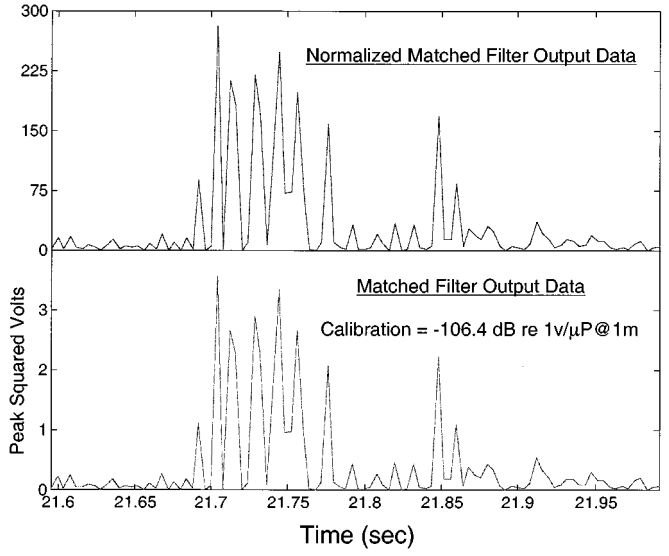

Fig. 16. Matched filter output before and after normalization.

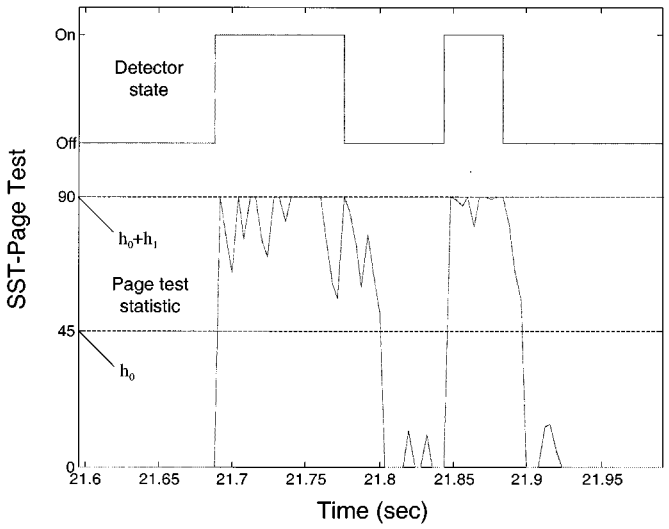

Fig. 17. Results of SST-Page test with design SNR estimated from sonar equation.

VI. Conclusion

A sequential detector based on the Page test, called the SST-Page test, has been proposed for the detection of active sonar echoes in shallow-water environments where propagation through the water and reflection off the target spread the transmitted signal in time. The proposed detector is tuned as a function of range to the estimated SNR to help suppress signal-like reverberation.

The probability of one or more false alarms while processing a full ping of data was introduced as an appropriate false alarm performance measure for active sonar systems. This false alarm performance measure was related to the PMF of the stopping time of an active sonar detector. The PMF of the stopping time of the proposed SST-Page test and the thresholded matched filter were determined. The theoretical false alarm performance of the SST-Page test, the standard Page test, and the thresholded matched filter were compared as a function of range where the false alarm suppression capability of the SST-Page test at short ranges was illustrated.

The theoretical detection performance of a finite duration signal for the Page test was derived when it was assumed that the Page test was initially in the steady state under the signal-absent hypothesis and when accounting for latent detections. The theoretical detection performance of the Page test was investigated as a function of signal duration, SNR, and for the SST-Page test as a function of range. It was observed that the Page test outperforms the thresholded matched filter except when the signal is extremely short.

An AH-Page test and the SST-Page test were used to process reverberation data known to contain reflections from a subseabottom geological feature. The SST-Page test was seen to suppress reverberation generated detections in the AH-Page test while still detecting the target-like geological feature.

Appendix I
Page Test False Alarm Performance

Evaluation of the false alarm performance for the Page test requires computation of the cumulative distribution function of the stopping time. As shown in [11], this may be accomplished by quantizing the update of the Page test, g_n^0, to equally spaced levels, say at intervals of width Δ. Arbitrarily, let the levels be $l_i = i\Delta$ for $i = 0, \pm 1, \pm 2, \ldots$. Define the probability of observing each state at time n (i.e., the Page test statistic takes on level l_i at time n) as $\{p_i^n\}$ under H_0 and as $\{q_i^n\}$ under H_1.

As described in [11], a probability transition matrix under H_0 including regulation at zero is formed as

$$\mathbf{C}_n = \begin{bmatrix} \sum_{i=-\infty}^{0} p_i^n & \sum_{i=-\infty}^{-1} p_i^n & \cdots & \sum_{i=-\infty}^{-(\gamma-1)} p_i^n \\ p_1^n & p_0^n & \cdots & p_{-\gamma+2}^n \\ p_2^n & p_1^n & \cdots & p_{-\gamma+3}^n \\ \vdots & \vdots & \ddots & \vdots \\ p_{\gamma-1}^n & p_{\gamma-2}^n & \cdots & p_0^n \end{bmatrix} \tag{30}$$

where γ is the integer satisfying $l_{\gamma-1} < h_0 \leq l_\gamma$.

If $\mathbf{u}_0$ is a vector composed of the initial probabilities of observing the continuing states $(l_0, l_1, \ldots, l_{\gamma-1})$, then the probability of observing the continuing states at time n is

$$\mathbf{u}_n = \mathbf{C}_n \mathbf{C}_{n-1} \cdots \mathbf{C}_1 \mathbf{u}_0. \tag{31}$$

The CDF of the stopping time is simply the probability that the test has stopped prior to or during the current time sample

$$\begin{aligned} F_N(n) &= \Pr\{N \leq n\} \\ &= 1 - \Pr\{\text{observing a continuing state at time } n\}. \end{aligned} \tag{32}$$

Premultiplying (31) by a row vector of ones provides the probability of observing a continuing state at time n. Thus, the CDF of the stopping time under H_0 is

$$F_N(n) = 1 - \mathbf{1}^T \mathbf{C}_n \mathbf{C}_{n-1} \mathbf{C}_{n-2} \cdots \mathbf{C}_1 \mathbf{u}_0 \tag{33}$$

where $\mathbf{1}$ is a vector of ones and the superscript T represents the transpose operation. In most applications, the detector will start from the zero state so $\mathbf{u}_0$ is a vector with a one in the first position and zeros elsewhere.

Appendix II
Page Test Probability of Detection

Assuming a constant bias in the Page test throughout the duration of the signal (and afterward for latent detections) and a signal with constant noncentrality parameter and duration L, the probability of detection is

$$P_d(L) = \Pr_1\{N \leq L\} + \Pr_0\{\mathcal{S}(\mathbf{v}_L)\} \tag{34}$$

where the subscripts on the probabilities indicate that they are taken when signal is present (1) or absent (0). Here, $\mathcal{S}(\mathbf{u})$ is the event that a threshold crossing occurs before a reset to zero when the probabilities of being in the nonzero continuing states $(l_1, l_2, \ldots, l_{\gamma-1})$ are the elements of the vector $\mathbf{u}$. The vector $\mathbf{v}_L$ is the probability of being in the nonzero continuing states after processing L samples containing signal

$$\mathbf{v}_L = \mathbf{P}\mathbf{C}_1^L \mathbf{u}_{ss} \tag{35}$$

where $\mathbf{P} = [\mathbf{0} \quad \mathbf{I}_{\gamma-1}]$ is a $\gamma - 1$ by γ matrix that isolates the probabilities of observing the nonzero continuing states, $\mathbf{u}_{ss}$ is

a vector of the steady-state probabilities of observing the continuing states $(l_0, l_1, \ldots l_{\gamma-1})$ under H_0, and $\mathbf{C}_1$ is the constant probability transition matrix including regulation at zero formed under H_1 (cf. (31) with q_i rather than p_i).

Similar to the development found in [15], the probability of a straight climb to the threshold from the nonzero continuing states may be shown to be the probability of a threshold crossing for each future time sample assuming the zero state is never entered

$$\begin{aligned}\Pr_0\{\mathcal{S}(\mathbf{v}_{\mathcal{L}})\} =& \sum_{k=0}^{\infty} \mathbf{c}_0^T \mathbf{D}_0^k \mathbf{v}_L \\ =& \mathbf{c}_0^T \left(\mathbf{I}_{\gamma-1} - \mathbf{D}_0\right)^{-1} \mathbf{v}_L \end{aligned} \tag{36}$$

where $\mathbf{D}_0$ is a transition probability matrix for the nonzero continuing states formed under H_0

$$\mathbf{D}_0 = \begin{bmatrix} p_0 & p_{-1} & \cdots & p_{-\gamma+2} \\ p_1 & p_0 & \cdots & p_{-\gamma+3} \\ \vdots & \vdots & \ddots & \vdots \\ p_{\gamma-2} & p_{\gamma-3} & \cdots & p_0 \end{bmatrix} \tag{37}$$

and $\mathbf{c}_0$ is a vector of the probabilities of crossing the threshold at the next update from each of the nonzero continuing states under H_0

$$\mathbf{c}_0 = \begin{bmatrix} \sum_{i=\gamma-1}^{\infty} p_i \\ \sum_{i=\gamma-2}^{\infty} p_i \\ \vdots \\ \sum_{i=1}^{\infty} p_i \end{bmatrix}. \tag{38}$$

Combining (34)–(36) and (33) with a constant transition probability matrix $(\mathbf{C}_1)$ results in

$$\begin{aligned} P_d(L) =& 1 - \mathbf{1}^T \mathbf{C}_1^L \mathbf{u}_{ss} + \mathbf{c}_0^T \left(\mathbf{I}_{\gamma-1} - \mathbf{D}_0\right)^{-1} \mathbf{P} \mathbf{C}_1^L \mathbf{u}_{ss} \\ =& 1 - \mathbf{b}^T \mathbf{C}_1^L \mathbf{u}_{ss} \end{aligned} \tag{39}$$

where

$$\mathbf{b}^T = \mathbf{1}^T - \mathbf{c}_0^T \left(\mathbf{I}_{\gamma-1} - \mathbf{D}_0\right)^{-1} \mathbf{P}. \tag{40}$$

Equation (39) may be interpreted as one minus the probability of not crossing the threshold before a reset to zero (the vector $\mathbf{b}$) given the detector is in a continuing state at the end of the signal $(\mathbf{C}_1^L \mathbf{u}_{ss})$. As noted in [11], inclusion of latent detections and allowing the Page test to be in the steady state under H_0 prior to the start of the signal is important for predicting the detection performance of weak and short to moderate duration signals.

REFERENCES

[1] R. J. Urick, *Principles of Underwater Sound*. New York: McGraw-Hill, 1983.

[2] P. M. Baggenstoss, "On detecting linear frequency-modulated waveforms in frequency- and time-dispersive channels: Alternatives to segmented replica correlation," *IEEE J. Ocean. Eng.*, vol. 19, pp. 591–598, Oct. 1994.

[3] E. S. Page, "Continuous inspection schemes," *Biometrika*, vol. 41, pp. 100–114, 1954.

[4] R. L. Streit, "Load modeling in asynchronous data fusion systems using Markov modulated Poisson processes and queues," in *Proc. Signal Processing Workshop*, Washington, DC, Mar. 24–25, 1995.

[5] G. Lorden, "Procedures for reacting to a change in distribution," *Ann. Math. Stat.*, vol. 42, no. 6, pp. 1897–1908, 1971.

[6] G. V. Moustakides, "Optimal stopping times for detecting changes in distributions," *Ann. Stat.*, vol. 14, no. 4, pp. 1379–1387, 1986.

[7] M. Basseville and I. V. Nikiforov, *Detection of Abrupt Changes: Theory and Applications*. Englewood Cliffs, NJ: Prentice-Hall, 1993.

[8] D. Brook and D. A. Evans, "An approach to the probability distribution of cusum run length," *Biometrika*, vol. 59, no. 3, pp. 539–549, 1972.

[9] B. Broder, "Quickest detection procedures and transient signal detection," Ph.D., Dep. of Elec. Eng., Princeton University, Princeton, NJ, 1990.

[10] C. Han, P. K. Willett, and D. A. Abraham, "False alarm time distributions in Page's test," in *Proc. 1995 Conf. Information Sciences and Systems*, Mar. 1995.

[11] ——, "Some methods to evaluate the performance of Page's test as used to detect transient signals," *IEEE Trans. Signal Processing*, vol. 47, pp. 2112–2127, Aug. 1999.

[12] H. L. Van Trees, *Detection, Estimation, and Modulation Theory: Part III*. New York: Wiley, 1971.

[13] P. P. Gandhi and S. A. Kassam, "Analysis of CFAR processors in nonhomogenous background," *IEEE Trans. Aerosp. Electron. Syst.*, vol. 24, pp. 427–445, July 1988.

[14] X. Macé de Gastines, "Robust Normalization Algorithms for Low-Frequency Active Sonar Signals," SACLANT Undersea Research Centre, La Spezia, Italy, SR-244, 1995.

[15] D. A. Abraham, "Analysis of a signal starting time estimator based on the Page test statistic," *IEEE Trans. Aerosp. Electron. Syst.*, vol. 33, pp. 1225–1234, Oct. 1997.

[16] ——, "Asymptotically optimal bias for a general nonlinearity in Page's test," *IEEE Trans. Aerosp. Electron. Syst.*, vol. 32, pp. 360–367, Jan. 1996.

[17] F. B. Jensen and M. C. Ferla, "SNAP: The SACLANTCEN Normal-Mode Acoustic Propagation Model," SACLANT Undersea Research Centre, La Spezia, Italy, SM-121, 1979.

[18] M. H. DeGroot, *Probability and Statistics*, 2nd ed. Reading, MA: Addison-Wesley, 1986.

[19] S. Kotz and N. L. Johnson, Eds., *Encylcopedia of Statistical Sciences*. New York: Wiley, 1985, vol. 6.

[20] N. L. Johnson, S. Kotz, and N. Balakrishnan, *Continuous Univariate Distributions*, 2nd ed: Wiley, 1995, vol. 2.

[21] M. Max, N. Portunato, and G. Murdoch, "Sub-Seafloor Buried Reflectors Imaged by Low Frequency Active Sonar," SACLANT Undersea Research Centre, La Spezia, Italy, SM-306, 1996.

Douglas A. Abraham was born in Bermuda in 1966. He received the B.S., M.S., and Ph.D. degrees in electrical engineering in 1988, 1990, and 1993, respectively, and the M.S. degree in statistics in 1994, all from the University of Connecticut, Storrs.

He is currently a Senior Research Associate with the Applied Research Laboratory of the Pennsylvania State University, State College. Previously he held a visiting faculty position at the University of Connecticut (1998–2000), was a Senior Scientist at the NATO SACLANT Undersea Research Centre in La Spezia, Italy (1995–1998), and was with the Naval Undersea Warfare Center in New London, CT (1989–1995). His work is primarily in the area of statistical signal processing applied to underwater acoustic applications. His current interests are in representing and accounting for non-Rayleigh active sonar reverberation in signal processing algorithms for detection, classification and localization.

Peter K. Willett received the B.A.Sc. degree from the University of Toronto, Toronto, ON, Canada in 1982 and the Ph.D. degree from Princeton University, Princeton, NJ, in 1986.

He is a Professor at the University of Connecticut, Storrs, where he has worked since 1986. His interests are generally in the areas of detection theory, target tracking and signal processing.

Prof. Willett is an Associate Editor for IEEE TRANSACTIONS ON SYSTEMS, MAN, AND CYBERNETICS, and also for IEEE TRANSACTIONS ON AEROSPACE AND ELECTRONIC SYSTEMS.